Earthq Eng & Eng Vib (2010) 9: 545-554 **DOI**: 10.1007/s11803-010-0036-y

Prediction of high-speed train induced ground vibration based on train-track-ground system model

Zhai Wanming†, He Zhenxing‡ and Song Xiaolin‡

Train and Track Research Institute, Traction Power State Key Laboratory, Southwest Jiaotong University, Chengdu 610031, China

Abstract: The development of analysis on train-induced ground vibration is briefly summarized. A train-track-ground integrated dynamic model is introduced in the paper to predict the ground vibration induced by high-speed trains. Representative dynamic responses of the train-track-ground system predicted by the model are presented. Some major results measured from two field tests on the ground vibration induced by two high-speed trains are reported. Numerical prediction with the proposed train-track-ground model is validated by the high-speed train running experiments. Research results show that the wheel/rail dynamic interaction caused by track irregularities has a significant influence on the ground acceleration and little influence on the ground displacement. The main frequencies of the ground vibration induced by high-speed trains are usually below 80 Hz. Compared with the ballasted track, the ballastless track structure can produce much larger train-induced ground vibration at frequencies above 40 Hz. The vertical ground vibration is much larger than the lateral and longitudinal components.

Keywords: high-speed railway; ground vibration; dynamic model; simulation; field experiment

1 Introduction

The emergence of high-speed trains is one of the most significant technological advances in the transportation industry over the last part of the 20th century and the beginning of the 21st century (Galvin and Dominguez, 2009). High-speed rail transportation is quickly becoming a popular form of mass transit throughout the world. In China, the Beijing-Tianjin intercity high-speed railway was put into operation in August of 2008. At the same time, many high-speed railways are being constructed in China, and plans are underway for more high-speed rail systems to be constructed in the next decade.

However, as the speed of the trains continues to increase, potential problems arise. The train-induced ground vibration is one of the most common concerns. It may contribute to passenger discomfort, or could potentially cause serious damage to the track and the train (Zhai *et al*., 2009). In addition, ground vibration induced by high-speed trains is a major environmental issue, since such vibration can cause annoyance to the inhabitants of surrounding buildings in the form of vibration or noise, and may affect nearby hospitals, historical sites and high-tech industries (or even damage buildings, which has been reported in the news). In the Czech Republic, cracks induced by the vibration of trains were initialized in ancient structures built with bricks and stones, and ancient churches, such as St. Thomas church, collapsed because of crack propagation in Prague. This kind of vibration is now regarded as one of the most severe public hazards. It was reported that railway lines in Italy were forced to be relocated in order to avoid the influence of track vibration on the water city of Venice and the leaning tower of Pisa. Unfortunately, it is difficult to circumvent the sites since tracks must be placed with large turning radii to avoid high centripetal accelerations on the train and passengers. Therefore, the prediction of high-speed train induced ground vibration is becoming increasingly important, and much attention has been given to this subject (Hall, 2003; Takemiya, 2003; Ditzel and Herman, 2004; Celebi, 2006; Galvin and Dominguez, 2007; Cai *et al*., 2008; Ju, 2009).

It is well known that when a train runs along the track, its dynamic loads can be transmitted to the track structure and subgrade via the wheel-rail contact, and can also excite vibrations of both the track and ground, which can in reverse influence the vibrations of the vehicle. The train, the track and the ground are essentially coupled with each other, which indicates that

Correspondence to: Zhai Wanming, Train and Track Research Institute, Traction Power State Key Laboratory, Southwest Jiaotong University, Chengdu 610031, China
Tel: 86-28-87601843
E-mail: wmzhai@swjtu.edu.cn
†Professor; ‡PhD

Supported by: National Natural Science Foundation of China Under Grant No. 50838006 and No. 50823004; the Traction Power State Key Laboratory of Southwest Jiaotong University Under Grant No. 2008TPL-Z05; the Science and Technology Department of Sichuan Province

Received February 1, 2010; **Accepted** September 18, 2010

it is necessary to systematically investigate the high-speed train induced ground vibrations from an integrated system point of view (Zhai *et al*., 2009). However, the comprehensive system includes many factors related to the characteristics of the train, the track, and the properties of the local foundation soil, which involves interdisciplinary study, such as vehicle engineering, structure engineering, geotechnical engineering and mechanics, etc. So far, the research on the integrated train-track-ground system, especially on the ground vibration due to the high-speed train, has been widely reported.

Previous researchers usually focused on the sub-problem of the total system, which can be divided into two weakly coupled issues. One is the vehicle-track coupled dynamics, from which the excitation of the ground vibration due to the high-speed train can be correctly determined. The other is the vibration responses of the ground and the nearby structure generated by the moving train loads, which are always simplified as axle loads instead of the real wheel/rail dynamic forces (Ditzel and Herman, 2004; Celebi, 2006; Galvin and Dominguez, 2007; Cai *et al*,, 2008). In addition, the wave propagation and soil-structure interaction are also involved.

The track dynamics and the wheel-rail dynamic interactions have been focused on for more than 140 years, especially in the last two decades. Until the 1990s, the rapid development of the computation technique made it possible to analyze the large and complicated vehicle-track coupled system's dynamics. A detailed model for investigating the vertical dynamics of an integrated vehicle-track coupled system was first established by Zhai (1991), Zhai and Sun (1994). Many research studies were then carried out on the vehicle-track system dynamics (Zhai *et al*., 1996; Sun *et al*., 2003; Zhai and Wang, 2006; Xu and Ding, 2006). A three-dimensional vehicle-track spatially coupled model can be found in a recent paper (Zhai *et al*., 2009), in which the vehicle subsystem and the track subsystem are coupled through a spatial wheel-rail coupling model that considers rail vibrations in the vertical, lateral and torsional directions (Chen and Zhai, 2004). A computer program named TTISIM was developed based on the 3-D model to predict the vertical and lateral dynamic responses of the vehicle-track coupled system (Zhai, 2007), including the dynamic wheel-rail forces. These forces can be regarded as the excitation in calculating train induced ground vibrations.

The ground vibration response under train loads is always related to wave propagation, which is significantly different from the traditional stress wave propagation in soil, as it concerns the soil-structure interaction. The simplest method in analyzing the dynamic response of the soil induced by the train is subject to the dynamic load obtained from the vibration source analysis to the soil surface directly. Since the early 1960s, vehicle loads have been treated as a quasi-static moving load, and the analytical solution of the steady-state dynamic response of a half space soil due to a moving load has been deduced by means of the integral transform (Eason, 1965; Gakenheimer and Miklowitz, 1969). And, a further study on the steady-state dynamic response of a half space soil due to a moving point load was carried out, in which the effect of the moving speed was discussed (Jiang *et al*., 2004). The distributing wheel load was adopted in the investigation by Krylov and Ferguson (1994), Krylov (1995) and Hung and Yang (2001). As actual soil consists of many different layers with different mechanical parameters, it is essential and significant to analyze the dynamic response of the layered-soil under different loads. An approach to analyze the stress and displacement of a layered viscoelastic half-space was presented by De Barrors and Luco (1994). The dynamic response of the layered-soil under harmonic load was investigated using a thin-layer element method by Grundmann *et al*. (1999), Sheng *et al*. (1999) and Xie *et al*. (2004).

However, these analytical results are difficult to apply to complicated cases in practical engineering. Numerical methods, such as the finite element method (FEM), can avoid the disadvantages of analytical methods. Great efforts have been made to ascertain the ground vibration induced by train loads with the numerical method. The classical FEM must be modified because the wave can reflect on the boundary of the finite domain, which will result in an undependable response. Coupling the FEM with a half infinite element method, with scaled boundary FEM or with a boundary element method that retains the advantages of each method and eliminates their disadvantages, leads to the combined FEM used widely (Hall, 2003; Yang and Hung, 2001; Yang *et al*., 2003; Ekevid and Wiberg, 2002; Takemiya, 2003; Takemiya and Kojima, 2003).

It can be seen from the review above that a comprehensive study of the ground vibration in the view of the integrated train-track-soil interaction is needed. The primary intention of this paper is to establish an integrated train-track-ground coupled dynamic model to predict the train induced ground vibration. The model is validated by some field experiments.

2 Train-track-ground system coupled model

The physical system under consideration consists of straight rails supported on a track structure, which in turn rest on the foundation soil. The vehicle-track dynamics is involved in the present study, which was always ignored or simplified in previous studies on train-induced ground vibration. A diagram of the train-track-ground system model is shown in Fig. 1. In the integrated model, the train-track subsystem and the subgrade subsystem are coupled at the interface according to the deformation coordination between the track bottom and the foundation soil. By using the theory

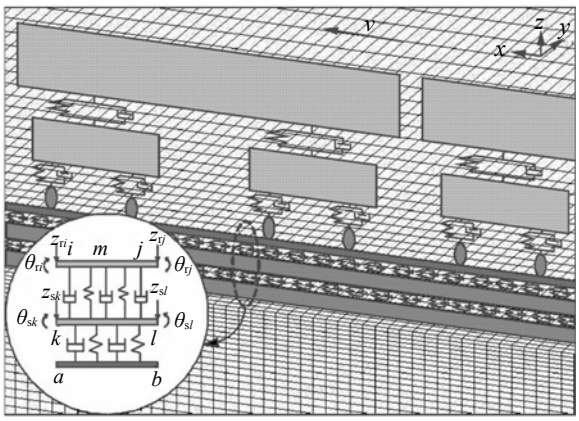

Fig. 1 Sketch of the train-track-ground system model

of vehicle-track coupled dynamics (Zhai, 2007; Zhai *et al*., 2009), the dynamic interaction between the train and the track, including the wheel-rail dynamic forces, can be calculated. The FEM is adopted to analyze the foundation soil region.

The total coordination system assumes that the x direction is along the railway longitudinal direction, the y direction is perpendicular to the railway, and z is in vertical direction.

2.1 Vehicle-track coupled model

The vehicle-track system model which was first presented in the early 1990s (Zhai, 1991; Zhai and Sun, 1994) consists of the vehicle sub-model and the track sub-model. In the vehicle sub-model, the car body is supported on two double-axle bogies at each end. The bogie frames are linked with the wheel sets through the primary suspensions and linked with the car body through the secondary suspensions. Spring-damper elements are used to represent the primary and secondary suspensions. The vehicle is assumed to move along the track at a constant traveling speed.

As the types of the track used in high-speed railways are multiform, the track sub-models are variable. In this paper, the ballastless slab track is considered because of its wide application in Chinese high-speed railways, which consists of rail, rail pad, slab, CA mortar, and concrete foundation, respectively. In the track sub-model, both the left and right rails are treated as continuous Bernoulli-Euler beams which are discretely supported at fastener junctions. The track slabs are described as elastic beams supported on a viscoelastic foundation. The vertical stiffness and damping of the CA layer are taken into consideration. The concrete foundation is considered to be rigid and assumed to rest directly on the free surface of the subgrade. If the analyzed track structure is not a slab track, such as the ballasted track, the above track dynamic model should be changed correspondingly (Zhai, 2007).

The wheel-rail coupling model is the essential element that couples the vehicle subsystem with the track subsystem at the wheel-rail interfaces. The Hertzian nonlinear elastic contact theory is used to calculate the wheel-rail dynamic forces in this paper.

2.2 FEM model of ground

The analysis based on FEM is performed to determine the 3D dynamic response of the ground induced by the high-speed train. The foundation soil region is modeled as a homogeneous linear elastic half space with a horizontal free surface. The concrete base of the slab track and the subgrade remain in contact all the time.

Due to symmetry, only half of the real subgrade needs to be modeled. The calculation time and the memory increase rapidly as the soil region size increases. It is impossible to simulate the dynamic response of the soil region when its size is too large. The length, width and thickness of the model are 70 m, 100 m and 50 m, respectively. The 3D viscoelastic dynamic artificial boundary conditions are applied to the boundaries of the model. Figure 2 shows an example of the shape and the mesh of the element. In order to obtain a more accurate solution, the maximum size of the 20-node solid element under the track is 0.5 m. The size increases with the increment of the distance away from the track, and the maximum size is no more than 3 m.

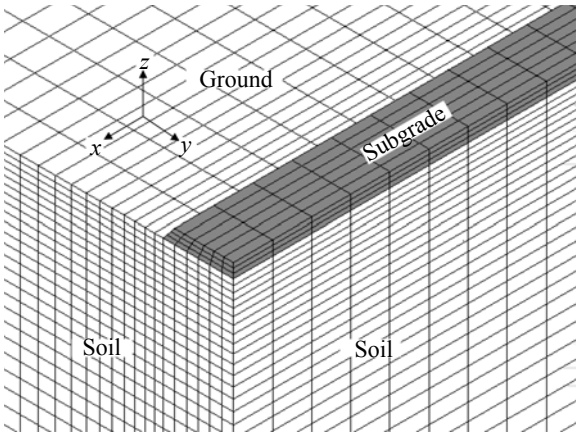

Fig. 2 Model and the mesh of the ground example

2.3 Coupled relationship between the train-track subsystem and the ground subsystem

As described above, the physical train-track-ground system consists of the vehicle-track coupled subsystem and the subgrade subsystem. The solution of the total system is divided into two parts, vehicle-track subsystem and subgrade subsystem, which are coupled through the deformation compatibility and force equilibrium of nodes at the track-subgrade interface.

The reaction force of the track bottom can be calculated by the vehicle-track coupled dynamics

theory in the vehicle-track subsystem. According to the compatibility condition of the force balance, the reaction force will be loaded on the corresponding nodes of the subgrade. In the subgrade subsystem, the displacement of the subgrade can be calculated by FEM, which will in reverse excite the deformation of the track structure. Therefore, the two subsystems are essentially coupled with each other.

In order to conveniently establish the coupling relationship between the track and the subgrade, the combined slab track element is adopted. In the combined element, the rail beam, track beam, and foundation beam are combined with a spring-damper, as shown in Fig. 3 and the enlarged view in Fig. 1. The discrete support of the fastener is equivalent to a continuous one to adapt for the element size of the subgrade. The foundation beam is assumed to be massless rigid. The combined slab track element is coupled with the subgrade element by Node *a* and Node *b*.

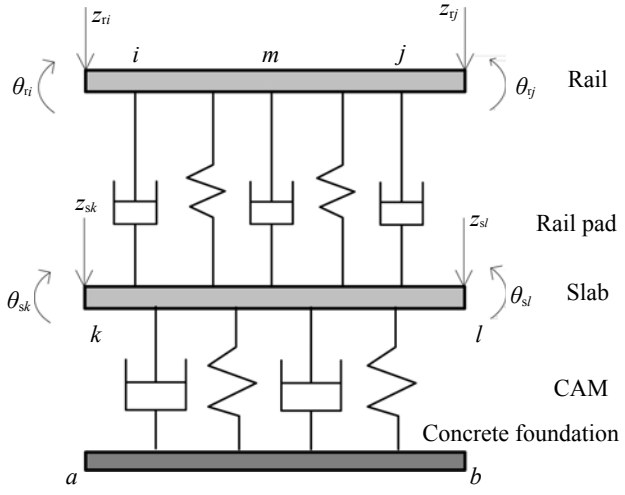

Fig. 3 Sketch of the combined slab track element

The combined element consists of two elastic beams, which involve four nodes: *i*, *j*, *k*, *l*. Each combined element has eight degrees of freedom (DOFs): z_{ri}, θ_{ri}, z_{rj}, θ_{rj}, z_{sk}, θ_{sk}, z_{sl}, θ_{sl}, where Z and θ are the vertical displacement and the rotation angle of the node. The displacement of the arbitrary point of the combined beam can be expressed as:

$$\boldsymbol{Z} = \boldsymbol{N}\boldsymbol{q}^{\mathrm{e}} \tag{1}$$

where $\boldsymbol{N}$ is the shape function matrix given by 3-order Hermite interpolation functions, and $\boldsymbol{q}^{\mathrm{e}}$ has the form of

$$\boldsymbol{q}^{\mathrm{e}} = \left(z_{ri}, z_{sk}, \theta_{ri}, \theta_{sk}, z_{rj}, z_{sl}, \theta_{rj}, \theta_{sl}\right)^{\mathrm{T}} \tag{2}$$

By means of the variation principle, the stiffness matrix of the combined element $\boldsymbol{K}_{\mathrm{r}}$, damping matrix of the combined element $\boldsymbol{C}_{\mathrm{r}}$ and mass matrix of the combined element $\boldsymbol{M}_{\mathrm{r}}$ can be deduced by the first variation of the system potential energy. These matrixes can be expressed as follows:

$$\boldsymbol{K}_{\mathrm{r}} = \sum \boldsymbol{K}_{\mathrm{b}i}^{\mathrm{e}} + \sum \boldsymbol{K}_{\mathrm{p}i}^{\mathrm{e}} + \sum \boldsymbol{K}_{ci}^{\mathrm{e}} \tag{3}$$

$$\boldsymbol{C}_{\mathrm{r}} = \sum \boldsymbol{C}_{\mathrm{p}i}^{\mathrm{e}} + \sum \boldsymbol{C}_{ci}^{\mathrm{e}} \tag{4}$$

$$\boldsymbol{M}_{\mathrm{r}} = \sum \boldsymbol{M}_{i}^{\mathrm{e}} \tag{5}$$

where $\boldsymbol{K}_{\mathrm{b}i}^{\mathrm{e}}$ is the element stiffness matrix of the rail and the slab; $\boldsymbol{K}_{\mathrm{p}i}^{\mathrm{e}}$ and $\boldsymbol{K}_{ci}^{\mathrm{e}}$ are the element stiffness matrices of the rail pad and the CAM; $\boldsymbol{C}_{\mathrm{p}i}^{\mathrm{e}}$ and $\boldsymbol{C}_{ci}^{\mathrm{e}}$ are the damping matrices of the rail pad and the CAM; and $\boldsymbol{M}_{i}^{\mathrm{e}}$ is the element mass matrix of the rail and the slab. Based on the principle of total potential energy with stationary value in elastic system dynamics, the final equations of the ballastless slab track can be described in terms of the standard matrix form as

$$\boldsymbol{M}\ddot{\boldsymbol{q}} + \boldsymbol{C}\dot{\boldsymbol{q}} + \boldsymbol{K}\boldsymbol{q} = \boldsymbol{F}(t) \tag{6}$$

where $\boldsymbol{M}$ is the mass matrix of the track structure; $\boldsymbol{C}$ and $\boldsymbol{K}$ are the damping and the stiffness matrices of the track system; $\ddot{\boldsymbol{q}}$, $\dot{\boldsymbol{q}}$ and $\boldsymbol{q}$ are the vectors of accelerations, velocity and displacement of the system, respectively; and $\boldsymbol{F}(t)$ is the node load vector of the track system.

3 Numerical results

By use of the train-track-ground coupled model, the dynamic responses of the track and the subgrade at any point can be obtained through numerical analysis. Dynamic responses of vehicles have been widely studied by researchers and will not be mentioned here.

As an example, ground vibration induced by a high-speed train with eight cars running on a slab track is investigated. Parameters of the vehicle and the track can be found in Zhai (2007). The subgrade is regarded as a homogeneous linear elastic body. The elastic modulus, density and Poisson's ratio are 45 MPa, 1800 kg/m^3 and 0.38, respectively. The train runs at a speed of 200 km/h. The track vertical geometry irregularity is considered.

3.1 Track and subgrade dynamic responses

Figures 4 and 5 show the predicted time histories of vertical accelerations of the track slab and the subgrade surface under the track, respectively. Very obvious impact can be found when each wheel passes through the observation site. The slab acceleration is much greater than the subgrade acceleration.

Figure 6 gives the time history of vertical displacement of the subgrade. Note that when the wheels pass through the rails, the vertical displacement of the subgrade increases remarkably and takes a peak value of about 4 mm in this case.

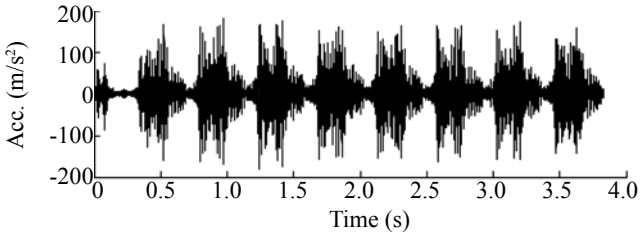

Fig. 4 Time history of vertical acceleration of track slab

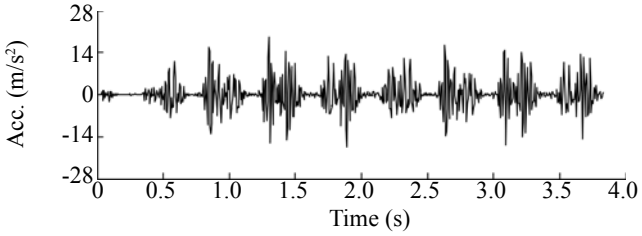

Fig. 5 Time history of vertical acceleration on the subgrade surface under the track

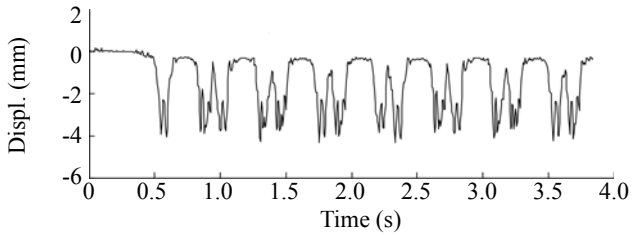

Fig. 6 Time history of vertical displacement of subgrade surface under the track

3.2 Ground vibration response

Figure 7 to Fig. 9 give the calculated time histories of displacement, velocity and acceleration of ground vibration, respectively. It can be seen that the peak responses in the vertical direction are always the largest and the peak responses in the longitudinal direction are the smallest among all the cases. The vertical waveform is somewhat similar to the lateral one, but the waveforms of the lateral response and the longitudinal one are quite different.

As is well known, it is important to understand the frequency characteristics of the responses in a study of environmental vibration problems. The investigation is focused here on the frequency components of the ground acceleration. The frequency spectra of the vertical, lateral and longitudinal accelerations of ground vibration at a point 15 m away from the track centerline are shown in Fig. 10. Note that the main frequencies are all focused in a narrow band below 10 Hz if the observation point is 15 m away from the track centerline. The dominant frequency is 2.4 Hz in all three directions. Other main frequencies are near 4.8 Hz and 7.2 Hz. Amplitudes in the frequency range of 10–30 Hz are very small.

When the observation point is changed, e.g., to 5 m away from the track centerline (originally 15 m in the case above), the calculated frequency spectra of ground accelerations are shown in Fig. 11. The main vibration frequency bands are generally below 80 Hz, much wider than before. The closer the distance between the observation point and the track centerline is, the stronger the high frequency vibration exhibits. This is because the

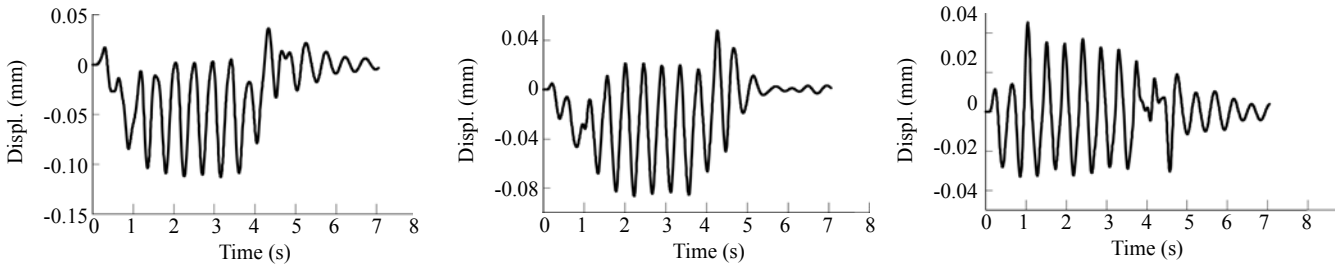

Fig. 7 Time histories of train-induced ground displacement (at a point of 15 m away from the track centerline)

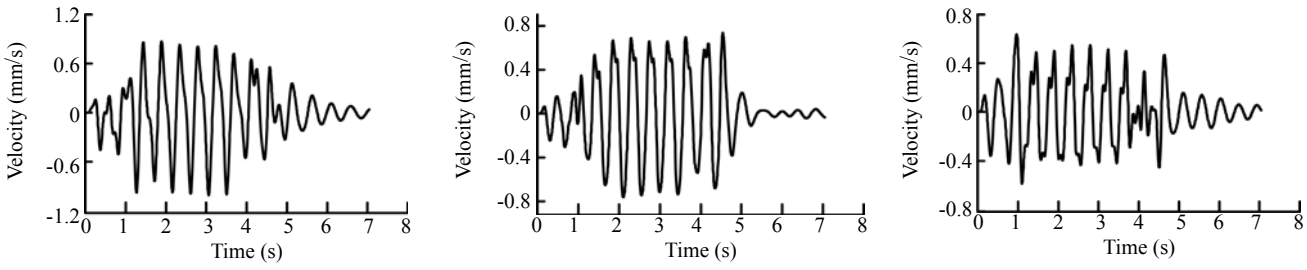

Fig. 8 Time histories of train-induced ground velocity (at a point of 15 m away from the track central line)

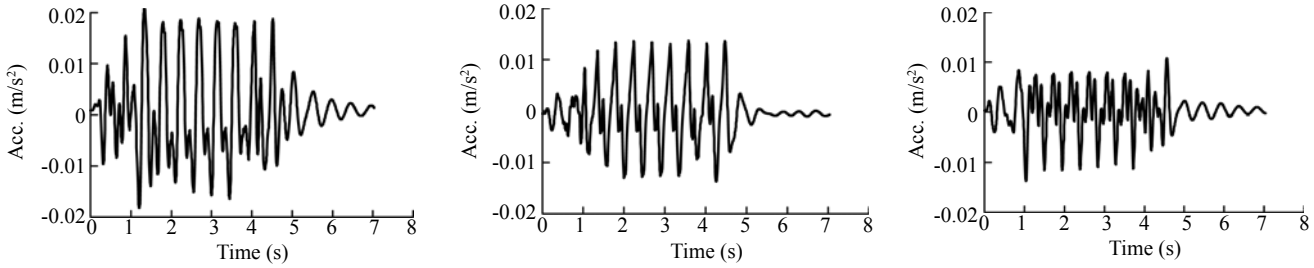

Fig. 9 Time histories of train-induced ground acceleration (at a point of 15 m away from the track centerline)

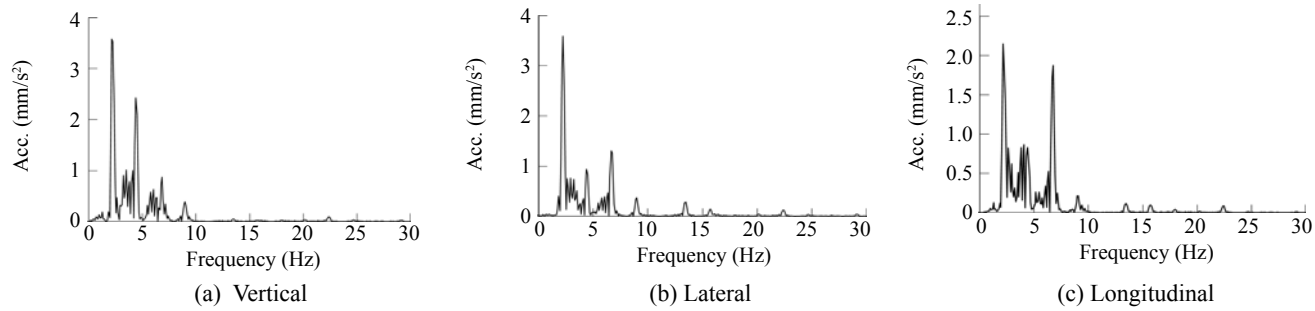

Fig. 10 Frequency spectra of train-induced ground acceleration (at a point of 15 m away from the track centerline)

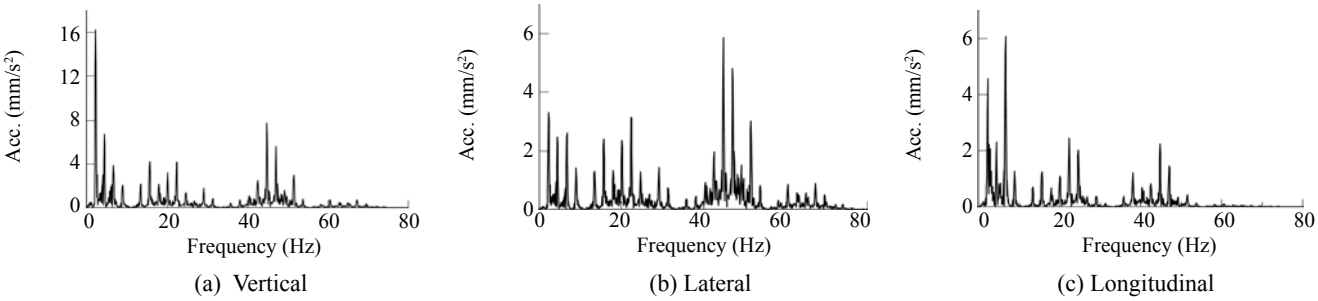

Fig. 11 Frequency spectra of train-induced ground acceleration (5 m away from the track centerline)

high-frequency vibrations in soil attenuate rapidly. The dominant frequency of the vertical acceleration is 2.4 Hz, while the dominant ones of the lateral and longitudinal accelerations are 45 Hz and 7.2 Hz, respectively, as shown in Fig. 11. It can be concluded from this calculation that the frequency spectra characteristics of the ground vibrations may be quite different at different locations away from the track centerline.

3.3 Comparison of the ground vibrations induced by static and dynamic wheel loads

As is well known, the static axle load is adopted by many researchers to simplify the analysis of the ground vibration. However, the axle load is not a real dynamic load. The dynamic load due to wheel-rail interaction may be much larger than the axle load, especially when the track geometry is not so good. How different are the results in the cases of these two loads? The calculated displacements and the accelerations of ground vibration under the static axle load and under the dynamic load are compared in Figs. 12 and 13, respectively, with the same track and ground conditions. The distance from the observation point on the ground to the track centerline is 5 m.

Figure 12 shows that the displacement of ground vibration under the static axle load is almost no different than from under the dynamic load. However, the ground acceleration under the dynamic load is obviously larger than under the static axle load, and the peak acceleration under the dynamic load is 10% to 20% larger than under the axle load, as shown in Fig. 13. Usually, the track irregularity can intensify the wheel/rail dynamic interaction, which has a significant effect on the ground vibration.

It can also be seen from Figs. 12 and 13 that the vertical ground vibration response is much larger than the lateral and longitudinal responses.

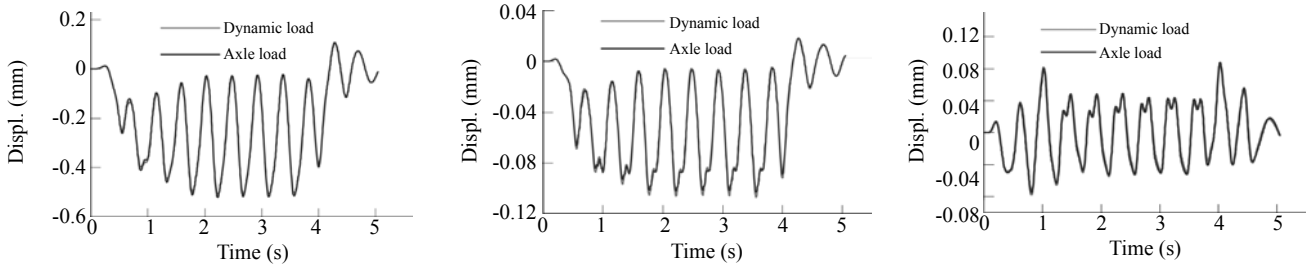

(a) Vertical (b) Lateral (c) Longitudinal

Fig. 12 Comparison of ground displacements under static axle load and dynamic load

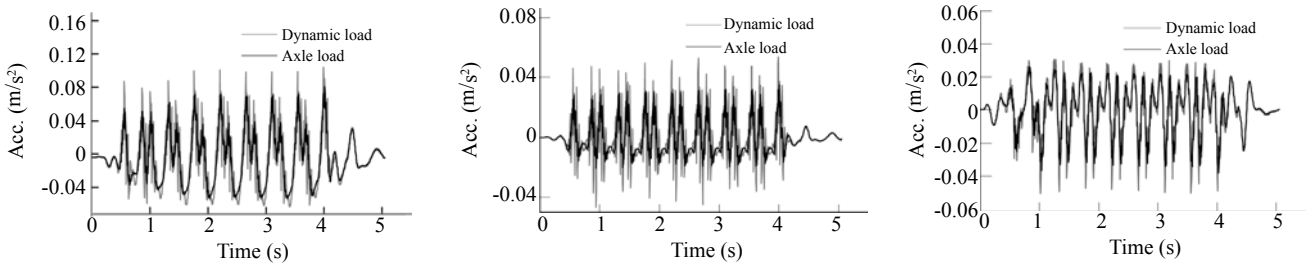

(a) Vertical (b) Lateral (c) Longitudinal

Fig. 13 Comparison of ground accelerations under static axle load and dynamic load

4 Field experiment

In this section, field measurements with different running speeds on two railway lines are briefly introduced. One is for a 200 km/h speed level test and the other is for a 300 km/h speed level test. Some typical results from the field tests as well as a comparison with computational results obtained from the train-track-ground coupled dynamics model are briefly reported. From this point forward, this study is restricted in the vertical vibration because it is much larger than the other two components, as illustrated from the results of the last section.

4.1 Case 1: ground vibration induced by a 300 km/h high-speed train

A field experiment on a high-speed railway line in China was carried out in June of 2008. The track structure on the tested section is a ballastless track with CHN 60 kg/m rails. The tested train is a high-speed Electric Multiple Unit (EMU) with test speeds from 180 km/h to 350 km/h. The parameters of the track slab and the CAM are shown in Table 1.

The vertical ground accelerations induced by the high-speed train with different running speeds are shown in Fig. 14. The ground vertical acceleration increases as the train speed increases and decreases with the addition of distance from the measured point to the track centerline. It is also indicated from Fig. 14 that the vibration attenuates rapidly as the distance increases to up to 20 m, and over this range, the vertical acceleration decreases slightly.

The frequency spectrum characteristics of the ground vibration induced by the high-speed train with different speeds are illustrated in Fig. 15. The maximum equivalent ground vibration levels at the speeds of 200 km/h, 250 km/h and 290 km/h are 61.59 dB, 67.73 dB and 68.75 dB, respectively, where the distance from the measured point to the track centerline is 30 m. The main vibration frequency is below 80 Hz, illustrating a rapid attenuation of high-frequency vibrations in the soil.

In Fig. 16, the relationships between the measured and the calculated ground vibration level attneuation are compared. It is shown that there is a good correlation between the measured data and calculated results, and the maximum difference of both results is only 4.2%.

Table 1 Parameters of slab track and CAM

Parameter	Elastic modulus (GPa)	Length (m)	Width (m)	Thickness (m)	Mass per unit length (kg/m)
Slab	35.5	6.45	2.55	0.2	1115.62
CAM	7.0	6.45	2.55	0.03	---

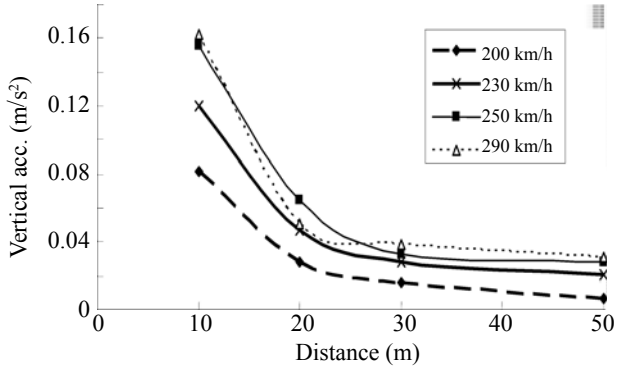

Fig. 14 Measured vertical ground acceleration attenuation

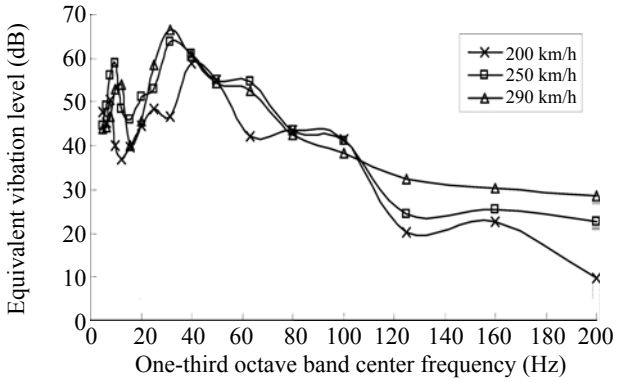

Fig. 15 Measured ground vibration frequency spectrum characteristics at different train speeds

4.2 Case 2: ground vibration induced by a Chinese 200 km/h EMU train

In 2007, the ground vibrations induced by a Chinese 200 km/h EMU train were measured on the Suining–Chongqing line by the China Academy of Railway Science (CARS). The vertical ground vibration levels at different train speeds are summarized in Table 2, in which the measurement point was located 30 m away from the track centerline. The track structure included the normal slab track, the vibration-reduced slab track and the bi-block track. Note that the bi-block track produced the highest ground vibration level, usually 6–7 dB higher than the normal slab track. Figure 17 gives a comparison of the frequency-dependent vibration levels measured on the ballast track and on the ballastless track for train speed of 200 km/h. A large difference is observed at the frequency above 40 Hz. The dominant ground vibration is in the frequency range of 20–80 Hz for the ballastless track and 20–50 Hz for the ballasted track. Figure 18 provides a comparison of the measured and calculated time histories of the ground vibration level. In this case, the measurement point was 7.5 m away from the track centerline. The tested track was a ballastless slab track, and the train running speed was 200 km/h. Note that the measured and calculated vibration levels are about 88–95 dB and 87–93 dB, respectively, i.e., the simulation being only approximately 3 dB less than the measurement.

Table 2 Vertical ground vibration levels at train speed of 160–220 km/h (CARS, 2007)

Train speed (km/h)	160	170	180	190	200	210	220
Normal slab track (dB)	75.0	75.0	76.5	77.0	77.0	77.5	78.0
Vibration-reduced slab track (dB)	77.5	77.5	78.0	78.0	79.0	79.0	79.0
Bi-block track (dB)	82.0	82.0	83.0	83.0	83.0	83.0	84.0

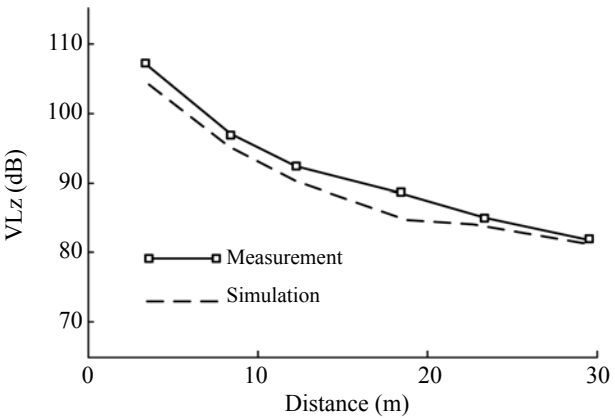

Fig. 16 Comparison of measured and calculated ground vibration level attenuation

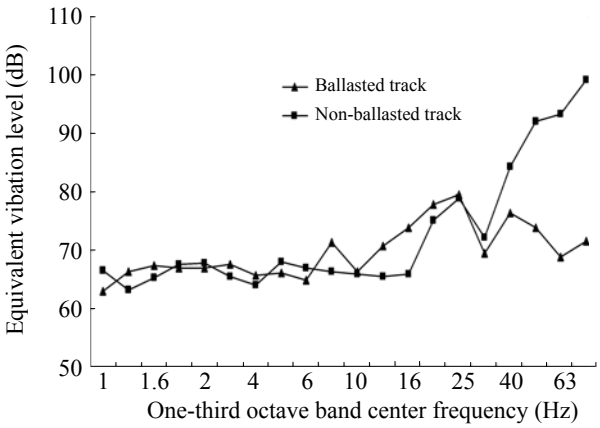

Fig. 17 Measured vertical ground vibration level induced by EMU on different tracks (Ma and Zhai, 2010)

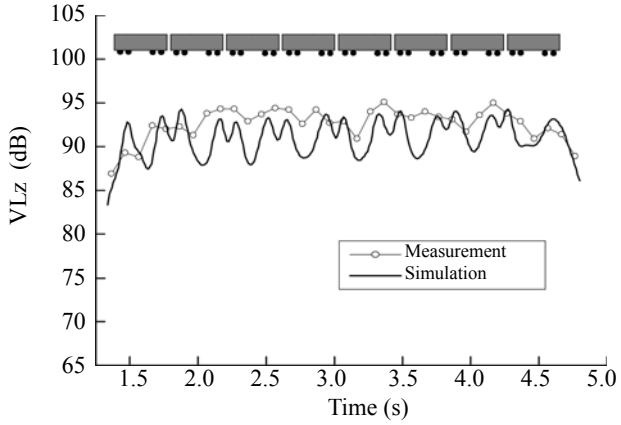

Fig. 18 Comparison of measured and calculated ground vibration levels

5 Conclusions

An integrated train-track-ground dynamic model has been presented on the basis of the vehicle-track coupled dynamics and the finite element method, in which the vehicle-track subsystem and the ground subsystem are coupled. Some major results from two field tests on the ground vibration induced by two high-speed trains have been introduced in the paper. Using the measured data, the train-track-ground dynamic system model has been primarily validated.

The results indicate that the influence of the wheel/rail dynamic interaction caused by track irregularities on the ground acceleration is significant. It is essential to consider the effect of the dynamic load in calculation of the ground acceleration induced by high-speed train. However, the dynamic wheel load has little influence on the ground displacement.

It can be summarized from both numerical results and experimental data that the train-induced ground vertical acceleration increases as the train running speed increases and decreases rapidly with the addition of the distance from the observation point to the track centerline. The vertical ground vibration response is much larger than the lateral and longitudinal responses.

The main frequencies of the ground vibration induced by high-speed trains are in the low frequency range, usually less than 80 Hz. Compared with the ballasted track, the ballastless track structure can produce much larger train-induced ground vibration at frequencies above 40 Hz.

Acknowledgement

This research was supported by the National Natural Science Foundation of China (NSFC) under grants No. 50838006 and No. 50823004, the Traction Power State Key Laboratory of Southwest Jiaotong University under grant No. 2008TPL-Z05, and also by the Science and Technology Department of Sichuan Province. The authors would like to thank the Scientific Committee of the 4th International Symposium on Environmental Vibration for recommending this paper to the journal.

References

Cai YQ, Sun HL and Xu CJ (2008), "Three-dimensional Analyses of Dynamic Responses of Track-ground System Subjected to a Moving Train Load," *Computers and Structures*, **86**: 816–824.

Celebi E (2006), "Three-dimensional Modeling of Train-track and Sub-soil Analysis for Surface Vibrations due to Moving Loads," *Applied Mathematics and Computation*, **179**: 209 –230.

Chen G and Zhai WM (2004), "A New Wheel/Rail Spatially Dynamic Coupling Model and Its Verification," *Vehicle System Dynamics*, **41**(4): 301–322.

China Academy of Railway Sciences (2007), *The General Report of the Test of the Non-ballasted Track Experimental Section on Suining-Chongqing Line*, Beijing. (in Chinese)

De Barros F and Luco J (1994), "Response of a Layered Viscoelastic Half-space to a Moving Point Load," *Wave Motion*, **19**:189–210.

Ditzel A and Herman GC (2004), "The Influence of a Rail Embankment on the Vibrations Generated by Moving Trains," *Journal of Sound and Vibration*, **271**: 937–957.

Eason G (1965), "The Stresses Produced in a Semi-Infinite Solid by a Moving Surface Force," *International Journal of Engineering Science*, **2**: 581–609.

Ekevid T and Wiberg NE (2002), "Wave Propagation Related to High-speed Train: a Scaled Boundary FE-approach for Unbounded Domains," *Computer Methods in Applied Mechanics and Engineering*, **191**: 3947–3964.

Gakenheimer DC and Miklowitz J (1969), "Transient Excitation of an Elastic Half Space by a Point Load Traveling on the Surface ," *Journal of Geotechnical Engineering*, ASCE, **36**(3): 505–515.

Galvin P and Dominguez J (2007), "Analysis of Ground Motion due to Moving Surface Loads Induced by High-speed Trains," *Engineering Analysis with Boundary Elements*, **31**: 931–941.

Galvin P and Dominguez J (2009), "Experimental and Numerical Analyses of Vibrations Induced by High-Speed Trains on the Cordoba–Malaga Line." *Soil Dynamics and Earthquake Engineering*, **29**: 641–657.

Grundmann H, Lieb M and Trommer E (1999), "The Response of a Layered Half-space to Traffic Loads Moving along Its Surface ," *Achieve of Applied Mechanics*, **69**: 55–67.

Hall L (2003), "Simulations and Analyses of Train-induced Ground Vibrations in Finite Element Models,"

Soil Dynamics and Earthquake Engineering, **23**: 403–413.

Hung HH and Yang YB (2001), "Elastic Waves in Wisco-elastic Half-space Generated by Various Vehicle Loads," *Soil Dynamics and Earthquake Engineering*, **21**: 1–17.

Jiang JQ, Zhou HF and Zhang TQ (2004), "Steady-state Response of an Elastic Half-space under a Moving Point Load," *Chinese Jounal of Geotechnical Engineering*, **26**(4): 440–444.

Ju SH (2009), "Finite Element Investigation of Traffic Induced Vibrations," *Journal of Sound and Vibration*, **321**: 837–853.

Krylov V (1995), "Generation of Ground Vibrations by Superfast Trains," *Applied Acoustics*, **44**: 149–164.

Krylov V and Ferguson C (1994), "Calculation of Low–frequency Ground Vibrations from Railway Trains," *Applied Acoustics*, **42**: 199–213.

Ma J and Zhai WM (2010), "Studies on Noise Vibration Characteristics of Ballastless Track and Addressing Measures," *Chinese Railways*, **17**(1): 31–37.

Sheng XZ, Jones C and Petyt M (1999), "Ground Vibration Generated by a Load Moving along a Railway Track," *Journal of Sound and Vibration*, **228**(1): 129–156.

Sun YQ, Dhanasekar M and Roach D (2003), "A Three-dimensional Model for the Lateral and Vertical Dynamics of Wagon-track Systems," *Journal of Rail and Rapid Transit*, **217**: 31–45.

Takemiya H (2003), "Simulation of Track-ground Vibrations due to a High-speed Train: the Case of X-2000 at Ledsgard," *Journal of Sound and Vibration*, **261**: 503–526.

Takemiya H and Kojima M (2003), "2.5D FEM Simulation for Vibration Prediction and Mitigation of Track and Ground Interaction under High-speed Trains," Chen and Takemiya, *Environmental vibration*. Beijing: China Communications Press, pp.130–138.

Xie WP, Wang GB and Yu YL (2004), "Dynamic Analysis of Soil Induced by Moving Load Based on Thin-layered Element Method," *Journal of Wuhan Urban Construction Institute*, **21**(2): 8–11. (in Chinese)

Xu YL and Ding QS (2006), "Interaction of Railway Vehicles with Track in Cross-winds," *Journal of Fluids and Structures*, **22** (3): 295–314.

Yang YB and Hung HH (2001), "A 2.5D Finite/infinite Element Approach for Modeling Visco-elastic Bodies Subjected to Moving Loads," *International Journal for Numerical Methods in Engineering*, **51**: 1317–1336.

Yang YB, Hung HH and Chang DW (2003), "Train-induced Wave Propagation in Layered Soils Using Finite/infinite Element Simulation," *Soil Dynamics and Earthquake Engineering*, **23**: 263–278.

Zhai WM (1991), "The Vertical Coupling Dynamics of Vehicle and Track as an Integral System," *Dissertation of Doctor Degree*, Chengdu: Southwest Jiaotong University. (in Chinese)

Zhai WM (2007), *Vehicle-track Coupling Dynamics*, 3rd ed, Beijing: Science Press. (in Chinese)

Zhai WM, Cai CB and Guo SZ (1996), "Coupling Model of Vertical and Lateral Vehicle/track Interactions," *Vehicle System Dynamics*, **26**(1): 61–79.

Zhai WM and Sun X (1994), "A Detailed Model for Investigating Vertical Interaction between Railway Vehicle and Track," *Vehicle System Dynamics*, **23**(Suppl.): 603–615.

Zhai WM and Wang KY (2006), "Lateral Interactions of Trains and Tracks on Small-radius Curves: Simulation and Experiment," *Vehicle System Dynamics*, **44**(Suppl.): 520–530.

Zhai WM, Wang KY and Cai CB (2009), "Fundamentals of Vehicle-track Coupled Dynamics," *Vehicle System Dynamics*, **49**(11): 1349–1376.